

# 고압 배터리 팩의 임피던스 스펙트럼 측정용 휴대용 임피던스 분광기

굴 라힘<sup>1</sup>, 최우진<sup>†</sup>

## A Portable Impedance Spectroscopy Instrument for the Measurement of the Impedance Spectrum of High Voltage Battery Pack

Gul Rahim<sup>1</sup> and Woo-Jin Choi<sup>†</sup>

### Abstract

The battery's State of Health (SOH) is a critical parameter in the process of battery use, as it represents the Remaining Useful Life (RUL) of the battery. Electrochemical Impedance Spectroscopy (EIS) is a widely used technique in observing the state of the battery. The measured impedance at certain frequencies can be used to evaluate the state of the battery, as it is intimately tied to the underlying chemical reactions. In this work, a low-cost portable EIS instrument is developed on the basis of the ARM Cortex-M4 Microcontroller Unit (MCU) for measuring the impedance spectrum of Li-ion battery packs. The MCU uses a built-in DAC module to generate the sinusoidal sweep perturbation signal. Moreover, it performs the dual-channel acquisition of voltage and current signals, calculates impedance using a Digital Lock-in Amplifier (DLA), and transmits the result to a PC. By using LabVIEW, an interface was developed with the real-time display of the EIS information. The developed instrument was suitable for measuring the impedance spectrum of the battery pack up to 1000 V. The measurement frequency range of the instrument was from 1 Hz to 1 KHz. Then, to prove the performance of the developed system, the impedance of a Samsung SM3 battery pack and a Bexel pouch module were measured and compared with those obtained by the commercial instrument.

**Keywords:** High voltage battery pack, EIS (Electrochemical Impedance Spectroscopy), AC impedance spectrum, DLA (Digital Lock-in Amplifier), ARM cortex-M4 microcontroller

### 1. Introduction

Li-ion batteries are widely used in large energy storage systems (ESS) such as energy storage power stations and electrical vehicles (EV) because of their advantages of high specific energy, high specific power, long cycle life and high charge-discharge efficiency. With the rapid expansion of the electric

vehicle market and as the core component of Electric Vehicles, batteries are drawing more attention. Battery performance directly affects the safety and reliability of the EV, so its managing technologies are quite crucial. Among them, the methods of estimating the state of health (SOH) and predicting remaining useful life (RUL) becomes the focus, which is essential to ensure their dependability and optimum performance over the time.

In most literature related to electric mobility, the end of life (EOL) for an EV battery is defined as a 20% drop of cell capacity from the nominal value<sup>[1]</sup>. But they can still store a large amount of energy and can operate in other applications that have been recently termed as second-life batteries (SLB). The lithium-ion batteries (LIBs) can be circulated as

Paper number: TKPE-2021-26-3-5

Print ISSN: 1229-2214 Online ISSN: 2288-6281

<sup>†</sup> Corresponding author: [cwj777@ssu.ac.kr](mailto:cwj777@ssu.ac.kr), Dept. of Electrical Engineering, Soongsil University, Korea  
Tel: +82-2-820-0652 Fax: +82-2-817-7961

<sup>1</sup> Dept. of Electrical Engineering, Soongsil University, Korea  
Manuscript received Dec. 15, 2020; revised Feb. 7, 2021;  
accepted Feb. 26, 2021

— 본 논문은 2020년 추계 학술대회 우수추천논문임

— 본 논문은 2020년 추계 학술대회 우수논문상 수상논문임

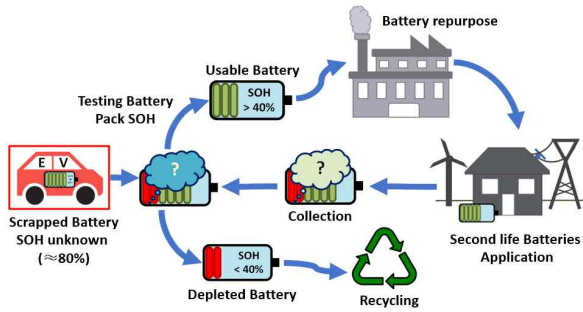


Fig. 1. Circulation of Li-ion batteries.

shown in Fig. 1. The used batteries from EVs are collected and the SOH of the battery pack is examined to estimate its remaining capacity, The battery is useful for second-life applications if the SOH of the battery is greater than 40% and it can be sent for repurposing. It can be broken down into modules or cells to make a new system for the SLB applications. The SLB modules or cells can be reconnected in series or parallel to obtain the required energy and power for a certain application. After the second-life the batteries are recycled to retrieve the raw materials.

To estimate the SOH of the batteries, EIS is one of the most attractive diagnostic techniques due to its convenience, quickness, and accuracy. EIS is a non-destructive technique that provides a considerable amount of information in a relatively short period<sup>[2]</sup>. The EIS technique can be used in various applications such as the quality assurance of the production line<sup>[3]</sup>, the state estimation of the battery including state of charge (SOC)<sup>[4]</sup>, SOH<sup>[5]</sup>, the internal temperature monitoring<sup>[6]</sup> and the estimation of RUL<sup>[7]</sup>. There are many advantages in using EIS for understanding the power delivery capability of Li-ion battery systems. It is a valuable tool utilized in different areas including applied chemistry, biomedical sciences, physical cells, and many other engineering fields. Electrical power sources such as fuel cell, supercapacitors and batteries can be modeled and diagnosed by this useful tool<sup>[8]</sup>. However, there are few commercially available EIS instruments developed so far, these instruments are quite expensive and designed to measure the low voltage batteries and have a long measuring time.

In this paper, a low-cost portable EIS instrument is developed, which can measure the impedance spectrum of the Li-ion battery packs up to 1000 V with no external power supply. While the conventional commercial instruments require external power to generate a sinusoidal perturbation current, the

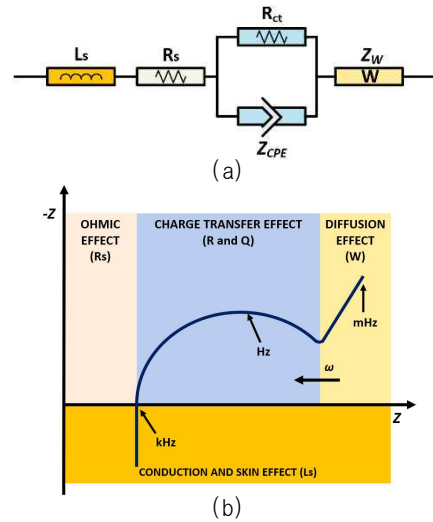


Fig. 2. (a) An ECM of LIB and (b) its nyquist plot.

proposed EIS instrument does not need it because the impedance spectrum of the battery is measured during the discharge only. It is advantageous in that the proposed instrument only requires a small power for the circuit operation which can be supplied through the USB cable. The system is composed of ARM Cortex-M4, high voltage protection circuit, signal conditioning circuit, and sensing circuit. graphical user interface (GUI) based on LabVIEW software was developed to display and evaluate the battery pack impedance. Due to the simplicity of the software, the operating personnel does not need complex training before they can accomplish measurement. The validity of the developed system is proved by comparing the measurement results obtained by the available “B” commercial instrument.

## 2. Development of the Portable EIS System

### 2.1 Electrochemical impedance spectroscopy

The EIS instrument measures the impedance spectrum of the battery with a small amplitude sine wave at different frequencies as a perturbation signal<sup>[9]</sup>. This provides useful information regarding the internal electrochemical processes inside the battery, which can be later used to extract the parameters of the equivalent circuit model (ECM) of the battery. In addition, useful information regarding aging, health, and capacity can be used to manage batteries for better performance and longer life cycles. An ECM of the battery is shown in Fig. 2(a). and the associated chemical reactions at different frequency regions of the Nyquist plot are shown in Fig. 2(b).

The high-frequency EIS is a straight line that reflects the inductive component of the battery and measurement apparatus. The cross point on the horizontal axis is the ohmic impedance ( $R_s$ ) which corresponds to the resistance of the electrolyte, electrodes, and wire used for the test. The aging of lithium-ion batteries is caused by a combination of various phenomena. Formation of microcracks, gas evolution, binder decomposition, corrosion of the current collector, and electrolyte depletion have all been reported as the cause of battery aging and performance degradation<sup>[10]</sup>. Hence it is challenging to distinguish these various processes and identify the characteristics of aging. In many cases, measuring the  $R_s$  using EIS would be a convenient method to evaluate the aging of the battery. The arc of the intermediate frequency region in the Nyquist plot is caused by the charge transfer resistance of  $\text{Li}^+$  at the interface between the electrode and the electrolyte and it is represented by a parallel circuit of charge transfer internal resistance ( $R_{ct}$ ) and Constant phase element ( $Z_{CPE}$ ) given by Eq. (1). Where  $Q$  is the time constant, and  $n$  is a real number between 0 and 1.  $R_{ct}$  has the largest value in the total cell resistance at room temperature and the power density of a lithium-ion battery is mainly dependent on  $R_{ct}$ . The low-frequency region is interpreted as the solid-state diffusion impedance represented by Warburg impedance ( $Z_W$ ) given by Eq. (2). Where  $Q$  is the mass transfer coefficient<sup>[11]</sup>.

$$Z_{CPE} = \frac{1}{(j\omega)^n Q} \quad (1)$$

$$Z_W = \frac{1}{Q\sqrt{j\omega}} \quad (2)$$

There are many kinds of different electrochemical analysis methods that can be used to investigate the internal processes of a battery. However, in the case of EIS analysis, it is possible to obtain important information from each component of an equivalent circuit model of a battery cell in a single experiment. Moreover, it is a non-destructive method that does not damage the battery. Additionally, it takes a relatively short time to carry out the measurement. If a precise circuit model is established, the parameter value of each component in the ECM of a lithium-ion battery can be obtained through analysis. Since the measurement can be easily carried out regardless of

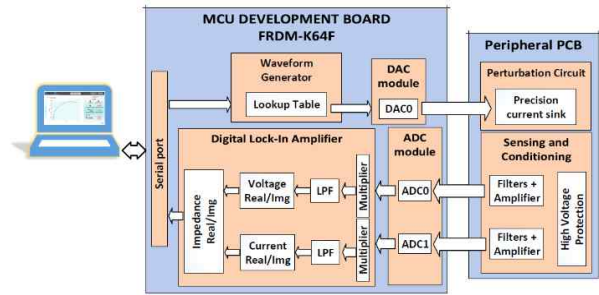


Fig. 3. Block diagram of the developed EIS system.

the size of the battery, the proposed EIS instrument can be an efficient analysis tool capable of investigating the degradation mechanisms of the LIBs<sup>[12]</sup>.

## 2.2 Hardware development

Fig. 3 shows the block diagram of the developed EIS system. The developed system is a plug and play device connected to the PC through the USB port and is controlled by LabVIEW. The main PCB board includes MCU, current control logic, high voltage protection, signal conditioning and sensing circuits. To perturb the battery pack 12-bit DAC of MCU is used to generate the sinusoidal sweep reference signal which is superimposed on a DC signal as shown in Eq. (3) and Eq. (4). The developed instrument has a frequency range from 1 Hz to 1 kHz with 6 and 3 frequencies per decade. The measured voltage and current signals are acquired from the battery pack by two separate 16-bit ADC's. For high accuracy of the acquired signal 200 kHz sampling frequency is used.

$$I_{pp} = I_p \sin(\omega t + \phi) + I_{dc} \quad (3)$$

$$I_{dc} > \frac{1}{2} I_{PP} \quad (4)$$

A high-precision current sink is used to control the perturbation current<sup>[13]</sup>. The control logic consists of a switch, a comparator, a current sensor, and an amplifier as shown in Fig. 4.

The gate voltage of the switch is controlled by taking feedback from the current sensor and comparing it with the input reference signal  $V_{ref}$  generated by the DAC. When a positive voltage is applied to  $V_{ref}$ , the output voltage of the comparator goes high, which turns on the switch and drives the current through the switch. As the current rises, the voltage on the current sensor also rises and the voltage feedback to the comparator increases until it

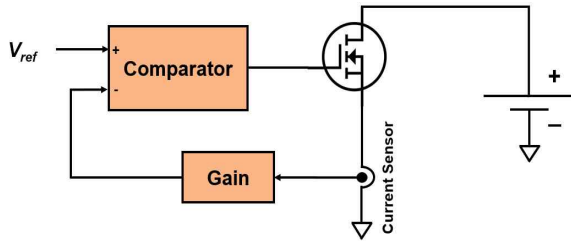


Fig. 4. High precision current sink.

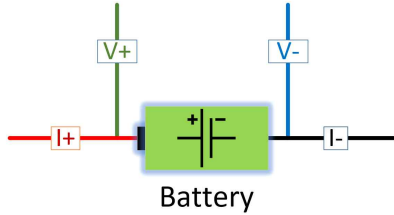


Fig. 5. Four-wire Kelvin connection.



Fig. 6. The front panel of the developed GUI.

is equal to  $V_{ref}$ . When the input signal at  $V_{ref}$  is sinusoidal it generates a sinusoidal current through the switch. The gain at the feedback decreases the sensitivity of the input reference signal.

The battery pack is connected to the developed EIS instrument using the Four-Wire Kelvin connection as shown in Fig. 5. The Four-Wire connector can eliminate the wire resistance and this structure can improve the accuracy of the measurement. The voltage across the battery is measured by using a passive high-pass filter and active low-pass filter which are used to block the DC and allow only filtered AC to be acquired by the ADC. The current is also sensed by the sensing resistor and amplified through the op-amp. With the acquired current and voltage data, only the required frequency component is extracted and the impedance at a certain frequency is calculated by the DLA.

### 2.3 Software development

The software for the developed system consists of an EIS algorithm based on DLA in the MCU and a GUI based on LabVIEW software as shown in Fig. 6.

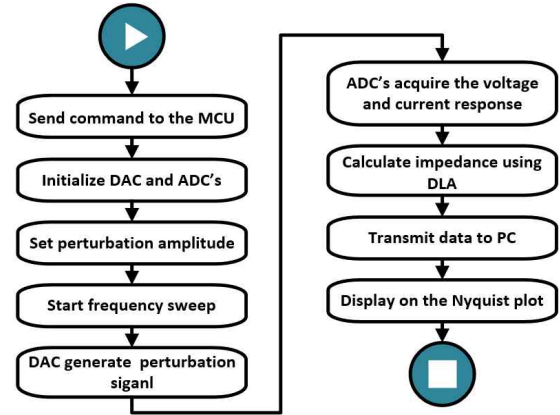


Fig. 7. Main program flowchart of developed system.

When the run button is pressed the system starts to generate a sinusoidal sweep signal with the desired magnitude to perturb the battery pack and the resulting current and voltage waveforms are acquired by MCU. The desired frequency component is extracted through DLA and the impedance of that specific frequency is plotted in real-time. The main program flowchart of the developed system is shown in Fig. 7.

The acquired signal is represented by Eq. (5), where  $A$  is the amplitude of the measured signal and  $\theta$  is the initial phase. the signal is discretized at the sampling frequency  $f_s = Nf$  where  $f$  is the frequency of the measured signal, and  $N$  is the number of samples. the sampling time interval is  $t_s = 1/(Nf)$ . The two reference signals are represented by Eq. (6) and Eq. (7), respectively, where  $B$  is the amplitude of the reference signal.

$$X_m[n] = A \sin\left(\frac{2\pi n}{N} + \theta\right) \quad (5)$$

$$r_1[n] = B \sin\left(\frac{2\pi n}{N}\right) \quad (6)$$

$$r_2[n] = B \cos\left(\frac{2\pi n}{N}\right) \quad (7)$$

When the measured signal is multiplied with two reference signals, a difference frequency term (DC signal) and a sum frequency term (double the reference signal frequency) are produced as shown in Eq. (8) and Eq. (9), respectively.

$$\begin{aligned} X_x[n] &= X_m[n] \bullet r_1[n] \\ &= \frac{AB}{2} \left[ \cos\theta + \cos\left(\frac{4\pi n}{N} + \theta\right) \right] \end{aligned} \quad (8)$$

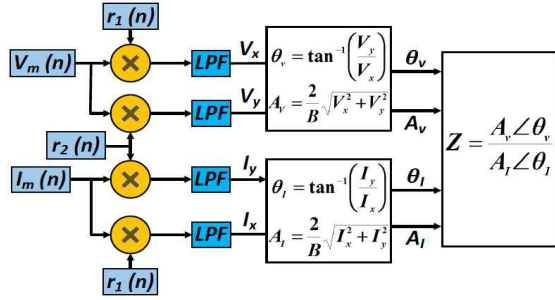


Fig. 8. Block diagram of the DLA to calculate impedance.

TABLE I  
BATTERY SPECIFICATIONS

Battery Type	Capacity	Nominal Voltage	Connection
Samsung SM3 Z.E	74 Ah	345.6 V	96s2p
Bexel 158309 Pouch Module	32 Ah	14.8 V	4s

$$X_y[n] = X_m[n] \bullet r_2[n] \quad (9)$$

$$= \frac{AB}{2} \left[ \sin\theta + \sin\left(\frac{4\pi n}{N} + \theta\right) \right]$$

The two outputs are passed through low pass filters to get the two DC signals as shown in Eq. (10) and Eq. (11), respectively.

$$X_x = \frac{AB}{2} \cos\theta \quad (10)$$

$$X_y = \frac{AB}{2} \sin\theta \quad (11)$$

The amplitude and phase of the acquired signal can be obtained by using Eq. (12) and Eq. (13) respectively. Two separate DLAs are used to obtain the amplitudes ( $A_v$  and  $A_I$ ) and phases ( $\theta_v$  and  $\theta_I$ ) of the acquired voltage and current signals. The impedance  $Z$  can be calculated by using Eq. (14). The block diagram of DLA to calculate impedance is shown in Fig. 8.

$$A = \frac{2}{B} \sqrt{X_x^2 + X_y^2} \quad (12)$$

$$\theta = \tan^{-1}\left(\frac{X_y}{X_x}\right) \quad (13)$$

$$Z = \frac{A_v \angle \theta_v}{A_I \angle \theta_I} \quad (14)$$

### 3. Experimental Results

To verify the performance and accuracy of the developed instrument experiments are performed by

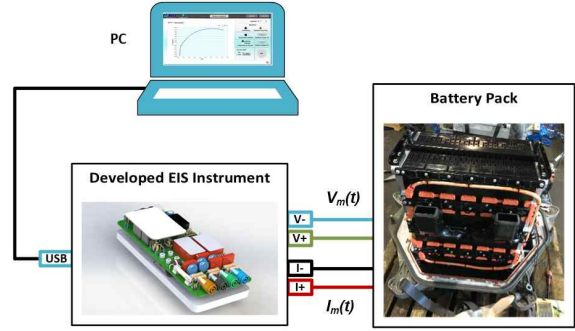


Fig. 9. Experimental setup.

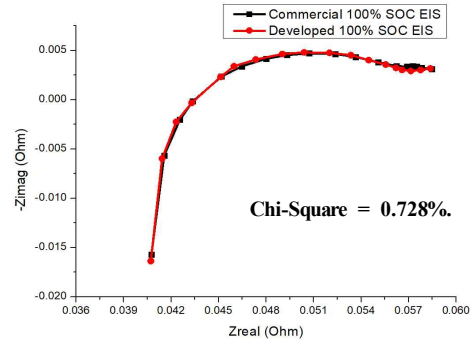


Fig. 10. Comparison of Nyquist impedance plot of Samsung SM3 Z.E battery pack measured by the developed system and commercial instrument.

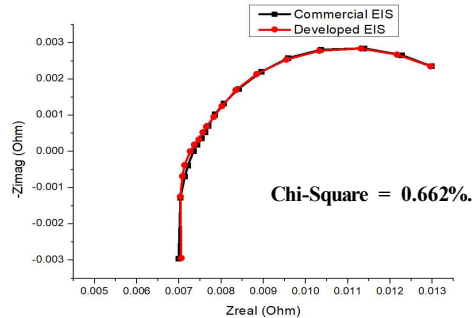


Fig. 11. Comparison of Nyquist impedance plot of Bexel pouch battery module measured by the developed system and commercial instrument.

measuring the impedance spectrum of the Samsung SM3 ZE battery pack and Bexel pouch module. The experimental setup is shown in Fig. 9, the developed EIS is connected to the PC and battery pack through a USB cable and a 4-wire Kelvin connection cable respectively. Table 1 shows the specifications of the battery pack and pouch module. A commercially available instrument is used for the comparison of the results to validate the developed instrument. As shown in Fig. 10, the measured impedance spectrum of the Samsung SM3 ZE battery pack by the developed instrument and commercial instrument has well-matched each other and shows the chi-square of 0.728%. Fig. 11 shows the results with the Bexel

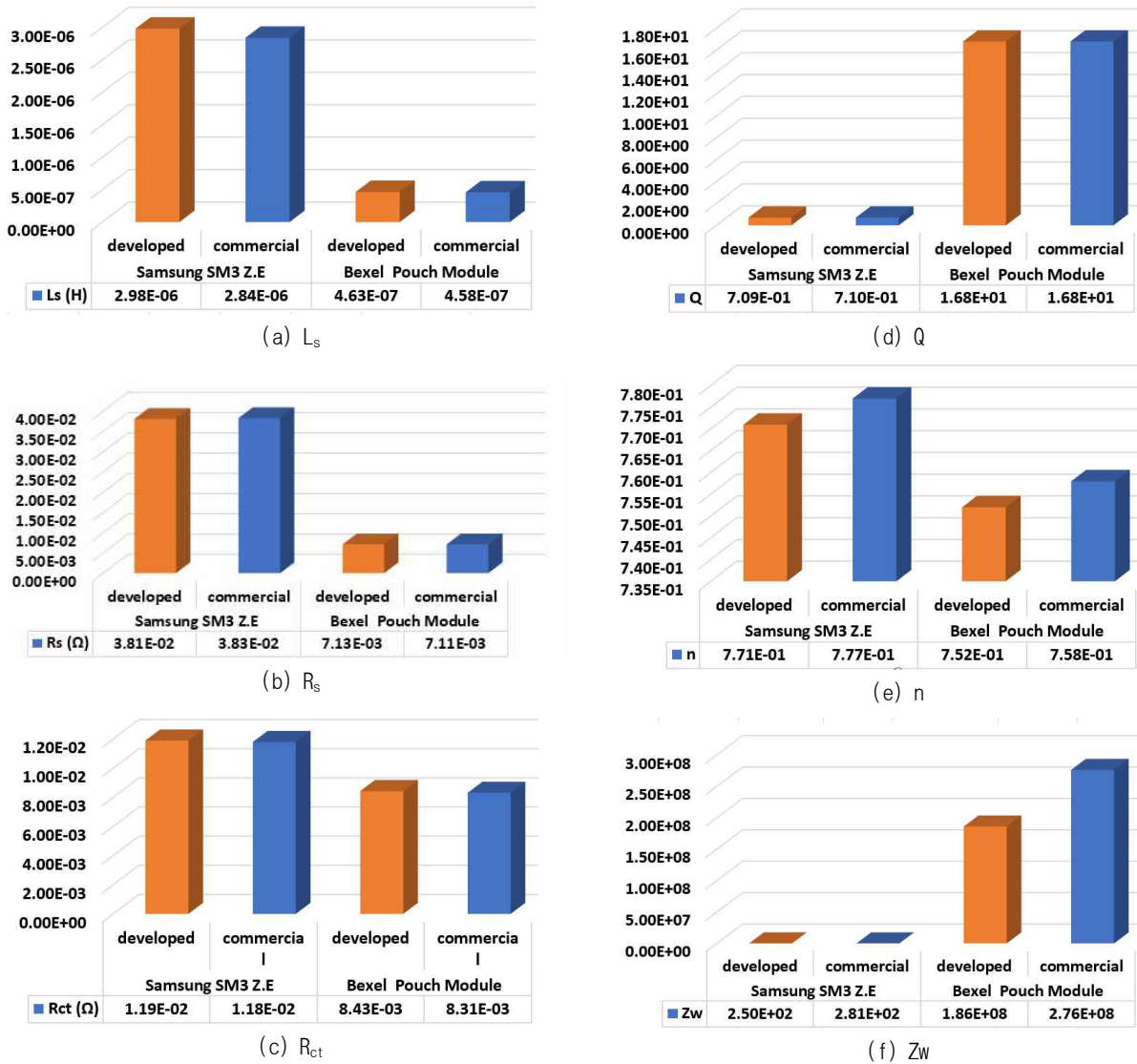


Fig. 13. Comparison of parameters of the ECM obtained by the developed and commercial instruments. (a)  $L_s$ , (b)  $R_s$ , (c)  $R_{ct}$ , (d)  $Q$  (e)  $n$ , (f)  $Z_w$ ,

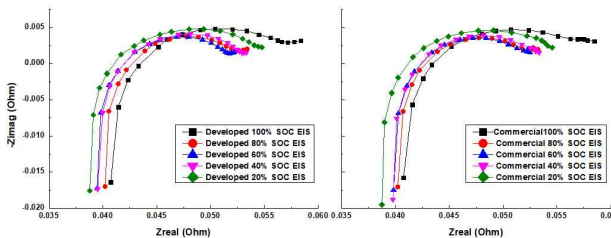


Fig. 12. Comparison of Nyquist impedance plot of Samsung SM3 Z.E battery pack measured by the developed system and commercial instrument at different SOC's.

pouch module with a chi-square of 0.662%. The Impedance spectrum of the Samsung SM3 ZE battery pack is also measured at different SOC's by discharging the battery pack. The comparison of the results with the commercial instrument is shown in Fig. 12. which are well-matched. The parameters extracted from the curve fitting with the ECM for

both the Samsung SM3 ZE battery pack and Bexel pouch module is shown in Fig. 13. It can be verified from the tests that the developed and commercial instrument shows almost the same results, thereby proving the measurement accuracy of the developed EIS instrument.

#### 4. Conclusions

In this paper, a portable EIS instrument that can measure the impedance spectrum of the Li-ion battery packs has been developed. The measurable frequency range is from 1 Hz to 1 kHz. The developed instrument can measure the impedance spectrum of the battery pack up to 1000 V and it can be utilized to evaluate the RUL of the EV battery pack for reuse. The experimental results show that the

developed instrument has good accuracy as the commercial instrument. The developed instrument uses a 5 V USB power supply only and does not require an external power supply. The developed instrument is a plug-and-play device and suitable for practical applications. Further work is in progress on this instrument to make the system faster, to reduce the measuring time because by shortened measurement time the EIS results will be more accurate.

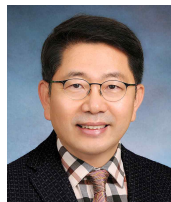
## References

- [1] R. Xiong and W. Shen, *Advanced battery management technologies for electric vehicles*, John Wiley & Sons, Inc., 2019.
- [2] U. Tröltzsch, O. Kanoun, and H. Tränkler, "Characterizing aging effects of lithium ion batteries by impedance spectroscopy," *Electrochimica Acta*, Vol. 51, No. 8/9, pp. 1664-1672, 2006.
- [3] K. Rumpf, M. Naumann, and A. Jossen, "Experimental investigation of parametric cell-to-cell variation and correlation based on 1100 commercial lithium-ion cells," *Journal of Energy Storage*, Vol. 14, pp. 224-243, 2017.
- [4] A. L. Rue et al., "State-of-charge estimation of LiFePO<sub>4</sub>-Li<sub>4</sub>Ti<sub>5</sub>O<sub>12</sub> batteries using history-dependent complex-impedance," *Journal of The Electrochemical Society*, Vol. 166, A4041, 2019.
- [5] X. Wang, X. Wei, and H. Dai, "Estimation of state of health of lithium-ion batteries based on charge transfer resistance considering different temperature and state of charge," *Journal of Energy Storage*, Vol. 21, pp. 618-631, 2019.
- [6] P. Haussmann, and J. Melbert, "Internal cell temperature measurement and thermal modeling of lithium ion cells for automotive applications by means of electrochemical impedance spectroscopy," *SAE International Journal of Electrified Vehicles*, Vol. 6, No. 2, pp. 261-270, 2017.
- [7] S. J. Lee, F. Farhan, A. Khan, and W. J. Cho, "AC impedance spectrum measuring device for battery modules to estimate the remaining useful life of lithium batteries," *The Transactions of the Korean Institute of Power Electronics*, Vol. 25, No. 4, pp. 251-260, 2020.
- [8] W. Choi and J. Lee, "Development of the low-cost impedance spectroscopy system for modeling the electrochemical power sources," in *2007 7th International Conference on Power Electronics, Daegu*, pp. 113-118, 2007.
- [9] A. Lasia, *Electrochemical impedance spectroscopy and its applications*, Springer-Verlag New York, 2014.
- [10] J. Vetter, P. Novák, M. R. Wagner, C. Veit, K. C. Möller, J. O. Besenhard, M. Winter, M. Wohlfahrt-Mehrens, C. Vogler, and A. Hammouche, "Ageing mechanisms in lithium-ion batteries," *Journal of Power Sources*, Vol. 147, No. 1/2, pp. 269-281, 2005.
- [11] Q. A. Huang, Y. Shen, Y. Huang, L. Zhang, and J. Zhang, "Impedance characteristics and diagnoses of automotive lithium-ion batteries at 7.5% to 93.0% state of charge," *Electrochimica Acta*, Vol. 219, pp. 751-765, 2016.
- [12] W. Choi, H. C. Shin, J. M. Kim, J. Y. Choi, and W. S. Yoon, "Modeling and applications of electrochemical impedance spectroscopy (eis) for lithium-ion batteries," *Journal of Electrochemical Science and Technology*, Vol. 11, No. 1, pp. 1-13, 2020.
- [13] M. Murnane, "Current sources: options and circuits," Application note AN-968 by analog devices. [Online]. Available at: <https://www.analog.com/media/en/technical-documentation/application-notes/AN-968.pdf>.



### Gul Rahim

He was born in Swat, Khyber Pakhtunkhwa, Pakistan in 1992. He received his B.S. degree from FAST National University of Computer and Emerging Sciences, Karachi, in 2015. He is currently pursuing his M.S. degree in Electrical Engineering from Soongsil University, Seoul, South Korea.



### Woo-Jin Choi

He was born in Seoul, South Korea, in 1967. He received the B.S. and M.S. degrees in Electrical Engineering from Soongsil University, Seoul, South Korea, in 1990 and 1995, respectively. He received his Ph.D. degree in Electrical Engineering from Texas A&M University, College Station, TX, USA, in 2004. He worked with Daewoo Heavy industries as Research Engineer, From 1995 to 1998. In 2005, he joined the School of Electrical engineering, Soongsil University. He is an Associate Editor of the IEEE Transactions on Industry Applications and an Executive Board Member of the Korean Institute of Power Electronics.